Wood Sci Technol
DOI 10.1007/s00226-014-0697-1

ORIGINAL

Changes in chemical and physical properties of yellow poplar (*Liriodendron tulipifera*) during torrefaction

Byeong-Il Na · Byoung-Jun Ahn · Jae-Won Lee

Received: 25 August 2014
© Springer-Verlag Berlin Heidelberg 2014

Abstract In this study, changes in the chemical and physical properties of yellow poplar were investigated during torrefaction. The torrefaction temperature was an important factor for changing the chemical compositions of the biomass. In particular, hemicelluloses were significantly affected by the torrefaction temperature. The torrefied biomass contained lower xylan and higher glucan and lignin concentrations than the raw material. The carbon content of the torrefied biomass increased from 44.80 to 52.96 % as the severity factor (SF), whereas the oxygen and hydrogen contents decreased from 45.08 to 36.77 and 5.89 to 5.62 %, respectively. The high carbon content in the torrefied biomass induced a decrease in the H/C and O/C ratios. The calorific value and weight loss increased proportionally to the SF. Under severe torrefaction conditions, the calorific value of the torrefied biomass was 20.84 MJ/kg, which represents an increase of 15.01 % compared to the raw material. Regarding the physical properties of the torrefied biomass, the moisture uptake capacity and specific energy consumption for grinding of biomass significantly decreased with increasing torrefaction severity. The torrefied biomass (55.1–65.6 kWh/t) required less energy than the raw material (145 kWh/t) for size reduction.

B.-I. Na · J.-W. Lee (✉)
Department of Forest Products and Technology, College of Agriculture and Life Sciences,
Chonnam National University, Gwang-ju 500-757, Republic of Korea
e-mail: ljw43376@chonnam.ac.kr

B.-J. Ahn
Division of Wood Chemistry and Microbiology, Department of Forest Products, Korea Forest
Research Institute, Seoul 130-712, Republic of Korea

Published online: 18 December 2014

Introduction

Recently, high prices of crude oil are causing an economic problem worldwide. It is clear that increasing demand and limiting supply of petroleum will sustain the rising prices and increase competition for secure petroleum supplies. To overcome this problem, biomass rather than fossil fuel is being increasingly utilized (Chen et al. 2011; Sims et al. 2006). In particular, lignocellulosic biomass plays an important role in the production of sustainable energy because it is renewable, abundant, relatively inexpensive, and often locally available. The currently high level of interest in lignocellulosic biomass conversion technology is driven by the potential of producing fuels and chemicals to reduce dependence on petroleum and reduce greenhouse gas emissions.

However, some specific properties of lignocellulosic biomass, such as high volatile content, high oxygen content, structural heterogeneity, low density, and high water content, present major obstacles for its use as an energy feedstock for solid fuel (Pala et al. 2014). Therefore, pretreatment technologies are needed to convert biomass into solid fuel. Many thermochemical conversion technologies, including carbonization, torrefaction, pyrolysis, and gasification, have been developed to treat lignocellulosic biomass (Chin et al. 2013; Lee et al. 2012; Pala et al. 2014).

Torrefaction is a mild thermal pretreatment process conducted in the temperature range of 200–300 °C under an inert or nitrogen containing atmosphere (Prins et al. 2006). This process generally results in approximately 10 % energy loss and 30 % weight loss depending on the torrefaction conditions (Peduzzi et al. 2014). Most of the hydroxyl groups and organic volatiles are removed from the biomass during torrefaction. Torrefaction provides hydrophobic conditions for the biomass, and the biomass becomes dry, darker, and brittle (Bourgeois et al. 1989). The torrefied biomass presents suitable chemical and physical characteristics for long-distance transportation and long-term storage. Additional, advantages of torrefaction include a higher calorific value and energy density with a low O/C ratio (Phanphanich and Mani 2011). Therefore, the torrefied biomass can be utilized as a solid fuel for home or industry use. It can also be co-fired with coal in a pulverized coal-fired boiler (Bergman et al. 2005).

Yellow poplar has been reported to acclimate well to barren soil and highlands. Its fast growth and high capacity for carbon absorption has led the Korea Forest Service to value this species as a major planting species, and it has thus been planted extensively in Korea for the production of woody biomass (Gwak et al. 2009). In this study, torrefaction was performed for yellow poplar under different temperatures and for different times. Additionally, the chemical and physical properties of biomass were investigated to understand the effect of the torrefaction process.

Materials and methods

Materials

Yellow poplar (*Liriodendron tulipifera*) chips were provided by Korea Forest Research Institute as lignocellulosic biomass and used for torrefaction. The wood chips were screened to the size of 10–30 mm using sieves (9.5 and 31.5 mesh) and dried to moisture content <10 %. The dried biomass was kept in a sealed plastic bag at room temperature for further processing.

Torrefaction process

The torrefaction of yellow poplar was performed at different temperatures (220–280 °C) and reaction time (20–80 min), which was expanded with four axial points and three replicates in the central point (Table 1). The severity factor (SF) was used to integrate the effects of reaction temperature and time into a single variable (Lloyd and Wyman 2005).

$$\text{Severity factor} = \text{Log}\left\{t \times \exp^{\left(\frac{T_h - T_r}{14.75}\right)}\right\} \tag{1}$$

where t is the reaction time for the torrefaction in minutes, T_h the reaction temperature (°C), and T_r the reference temperature, most often 100 °C.

Prior to torrefaction, the wood chips were dried at 105 °C for 24 h to remove the water from the biomass. The dried wood chips were placed in a torrefaction reactor, equipped with a temperature controller and stirring system (Drying Engineering Inc., Korea). The biomass was torrefied under each condition in the absence of oxygen by feeding nitrogen into the reaction with a flow of 2 ml/min. After reaching

Table 1 2^2 factorial design with four axial points and three replicates in the central point matrix employed for two independent variables

Sample no.	Variables		Coded levels		Severity factor (SF)
	Time (min) X_1	Temperature (°C) X_2	Time x_1	Temperature x_2	
1	50	250	0	0	6.12
2	50	250	0	0	6.12
3	50	250	0	0	6.12
4	70	270	1	1	6.85
5	70	230	1	−1	5.67
6	30	270	−1	1	6.48
7	30	230	−1	−1	5.30
8	80	250	1.4	0	6.32
9	50	280	0	1.4	7.00
10	20	250	−1.4	0	5.72
11	50	220	0	−1.4	5.23

the desired reaction temperature, the biomass was kept for each reaction time, and then, the heater was turned off. The torrefied biomass was collected and weighed.

Moisture content, elemental analysis, and calorific value of biomass

The moisture content, elemental and calorific value of the raw material and torrefied biomass were analyzed according to the quality standard of the wood pellet (Korea Forest Service 2009). The moisture content of the biomass was determined using the oven-dry method. The elemental analysis was conducted using an elemental analyzer (Thermo EA1112A, USA). Calorific values were measured using a Parr 6400 automated isoperibol bomb calorimeter (Parr Instrument Inc., USA).

Chemical compositions of biomass

The chemical composition of the raw material and torrefied biomass was determined according to National Renewable Energy Laboratory protocols (determination of carbohydrates and lignin content in biomass) (NREL, Golden, CO, USA). All experiments were performed in triplicate, and the mean value was reported.

Physical properties of biomass

To evaluate the grindability properties of the torrefied biomass, the size distribution of the biomass and power consumption during grinding was investigated. The torrefied biomass was placed into a four-blade cracker, and grinding was performed at 24,000 rpm for 1 min. The ground biomass was passed through three different sieves (1, 0.425 and 0.25 mm), and the fractions were separated and weighed depending on particle size. Energy consumption for size reduction in biomass was determined using an electronic energy meter (KEM2500, Korins Inc., Korea) during grinding. This energy only corresponds to that required for size reduction and not for movement of the mill alone.

Hydrophobic testing was performed to compare the moisture uptake capacity of raw material and torrefied biomass (Ibrahim et al. 2013; Pimchuai et al. 2010). Approximately 0.5 g of biomass was immersed in water for 2 h, followed by air drying for 1 h. Finally, the moisture content was measured.

Fourier transform infrared spectroscopy (FT-IR) was performed to study the functional group changes in torrefied biomass using a Nicolet 6700 spectrometer (Thermo Scientific, USA) with a universal ATR (window ZnSe/diamond). The spectrum was recorded in the wavelength range of 4,000–650 cm^{-1} with a resolution of 8 cm^{-1}.

The torrefaction characteristics of biomass were analyzed with a thermogravimetric analyzer (TA Instruments, USA). The heating temperature in the analyzer ranged from 25 to 700 °C with a heating rate of 10 °C/min. In each test, the biomass was tested under nitrogen gas flow of 100 ml/min. Both thermogravimetric and differential temperature measurements were recorded during combustion.

Measurement of the crystallinity value in the torrefied biomass was carried out via X'pert Pro Multipurpose X-ray Diffractometer (Panalytical, The Netherlands), as described by Segal et al. (1959).

Response surface analysis for chemical composition of biomass

A 2^2 factorial design was used to analyze the torrefaction characteristics of lignocellulosic biomass. The glucan, xylan, and lignin contents were used as the dependent output variables. Second-degree polynomials were calculated using Design-Expert version 8.0.1 software (Stat-Ease Inc., USA) to estimate the response of the dependent variables. Factors from each run were appropriately coded to real independent variables x_1 and x_2 for the statistical model, as shown in Table 1.

Results and discussion

Elemental properties and chemical composition of raw material and torrefied biomass

The moisture content of the biomass ranged from 1.34 to 3.62 %, whereas that of the raw material was 6.30 %. The concentration decreased with increase in SF (data not shown).

The elemental properties of the biomass are listed in Table 2. The carbon content of the torrefied biomass increased as the SF increased, whereas the oxygen and hydrogen content decreased. The increase in carbon content in a given biomass implies the improvement of fuel energy because carbon content is directly related to the calorific value (Klinger et al. 2013; Medic et al. 2012). The nitrogen content did not significantly change during torrefaction, which was expected as reduction in the hydroxyl groups with water vapor formation from the biomass typically occurs during torrefaction (Ibrahim et al. 2013).

Table 2 Elemental analysis of raw material and torrefied biomass (unit: %)

Severity factor	C (%)	H (%)	O (%)	N (%)
Raw material	44.80	5.89	45.08	0.23
5.23	46.76	5.97	41.96	0.21
5.30	47.12	5.89	43.24	0.24
5.67	47.50	5.93	42.43	0.20
5.72	48.54	5.98	39.79	0.25
6.12	49.23	5.92	40.02	0.20
6.32	50.14	5.84	38.51	0.27
6.48	51.79	5.75	30.89	0.23
6.85	52.12	5.77	36.72	0.23
7.00	52.96	5.62	36.77	0.22

The H/C atomic ratio was plotted against the O/C atomic ratio for the raw material and torrefied biomass including typical data points for lignite and anthracite, as shown in Fig. 1 (Ibrahim et al. 2013; Lee and Lee 2014). The higher carbon content in the torrefied biomass may have resulted in a decrease of the H/C and O/C ratios. Both the H/C and O/C ratios decreased as the SF increased. The composition of the torrefied biomass approached that of lignite. The tendency revealed in this study concerns dehydration, as the H/C atomic ratio is proportional to the O/C atomic ratio. This result agrees with other data from previous studies (Lee et al. 2012; Wen et al. 2014).

The glucan, xylan, and total lignin content of the biomass depended on the torrefaction conditions listed in Table 3. Xylan in the biomass was degraded during torrefaction. At a high SF (7.0), xylan content was only 6.14 % in the biomass. This result indicates that hemicelluloses are significantly affected by torrefaction. Hemicelluloses are known to decompose at a temperature of 225–300 °C (Prins et al. 2006); therefore, hemicelluloses degradation occurred regardless of the SF in this study. The amount of acetyl group also decreased with the xylan content because the xylose residues frequently contain approximately 7 acetyl groups per 10 xylose units in hardwood (Sjöström 1981). The hemicelluloses content in biomass has been confirmed as an important factor for torrefaction because the hemicelluloses content is directly related to the H/C and O/C ratios and hydrophobic properties (Bergman et al. 2005; Chin et al. 2013). In contrast, the concentration of glucan and lignin increased with the severity of torrefaction because of the degradation of hemicelluloses. Cellulose and lignin are thermally stable compared to hemicelluloses and are degraded at temperatures of 305–375 and 250–500 °C, respectively (Prins et al. 2006). High lignin content in torrefied biomass is associated with high energy density because of the ether and C–C linkages in lignin, which have a higher energy than C–O and C–H bonds (Shafizadeh et al. 1976; Lehtikangas 2001). Acid-insoluble lignin includes some products derived from the

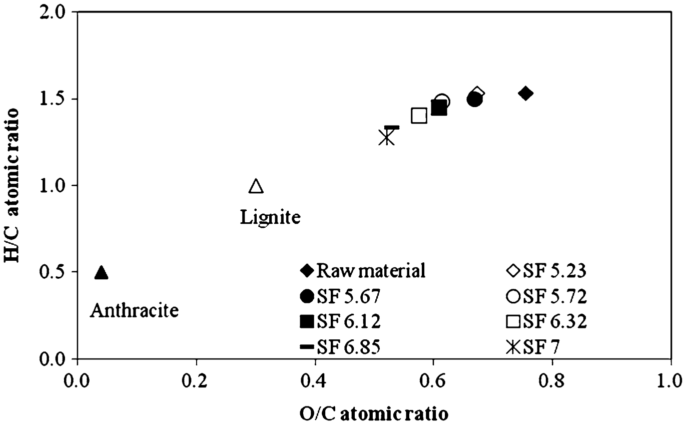

Fig. 1 H/C versus O/C atomic ratio of raw material and torrefied biomass depending on the torrefaction severity

Table 3 Chemical composition of raw material and torrefied biomass (unit: %)

Severity factor	Glucan	Xylan	Acetyl group	Acid-insoluble lignin	Acid-soluble lignin
Raw material	37.8 (0.90)	18.7 (0.36)	3.21 (0.11)	21.49 (0.75)	3.27 (0.07)
5.23	39.93 (0.70)	18.29 (0.28)	3.37 (0.07)	23.12 (0.36)	2.65 (0.74)
5.30	40.09 (0.93)	17.67 (0.72)	3.24 (0.08)	23.15 (0.74)	2.76 (0.03)
5.67	42.69 (0.69)	16.6 (0.25)	3.17 (0.26)	24.46 (0.98)	2.70 (0.03)
5.72	43.07 (1.04)	15.47 (0.30)	2.62 (0.36)	27.23 (0.82)	2.38 (0.27)
6.12	45.77 (0.42)	13.64 (0.71)	2.33 (0.07)	28.93 (0.45)	2.35 (0.10)
6.32	46.49 (1.21)	11.47 (0.60)	1.96 (0.04)	32.92 (0.63)	2.25 (0.04)
6.48	47.6 (0.61)	9.07 (0.15)	1.72 (0.08)	37.00 (0.24)	2.15 (0.21)
6.85	47.03 (0.91)	7.15 (0.17)	1.57 (0.10)	38.79 (1.40)	1.96 (0.33)
7.00	48.34 (0.84)	6.14 (0.16)	1.34 (0.16)	41.22 (0.45)	1.48 (0.14)

degradation of carbohydrate (Sannigrahi et al. 2011). Degradation products of carbohydrate such as furfural can react with lignin phenolic compounds, giving some acid-insoluble compounds during torrefaction (Chin et al. 2013). Therefore, torrefied biomass with low xylan and high glucan and lignin concentration is a suitable resource for improvement of fuel properties.

Response surface analysis for glucan, xylan, and lignin contained in the biomass

To determine appropriate torrefaction conditions for high glucan and lignin and low xylan content in the torrefied biomass, response surface analysis was performed. The modeling results for glucan, xylan, and lignin are given in Fig. 2. A three-dimensional plot was used to predict the concentration of each component under optimum conditions. The results of the analysis of variance (ANOVA) for Eqs. (2)–(4) are presented in Table 4. Y_1, Y_2, and Y_3 are the predicted concentration of glucan, xylan, and lignin, respectively. x_1 and x_2 denote the reaction time and temperature, respectively. These models were found to be significant at the 99 % confidence level. The model's F values for glucan (160.56), xylan (122.48), and lignin (51.35) were lower than the tabular F values, indicating that the models were significant in the region studied. For all models, the ''lack of fit F values'' was between 1.95 and 8.70, which implied that the lack of fit was not significant relative to the pure error. To fit the models, the lack of fit needs to be nonsignificant.

$$\begin{aligned} Y_1 = {} & 46.7667 + 3.0929x_2 + 0.7333x_1 \\ & - 0.5425x_1x_2 - 1.4046x_2^2 - 1.0821x_1^2 \end{aligned} \tag{2}$$

$$Y_2 = 13.07 - 4.5291x_2 - 0.9559 \tag{3}$$

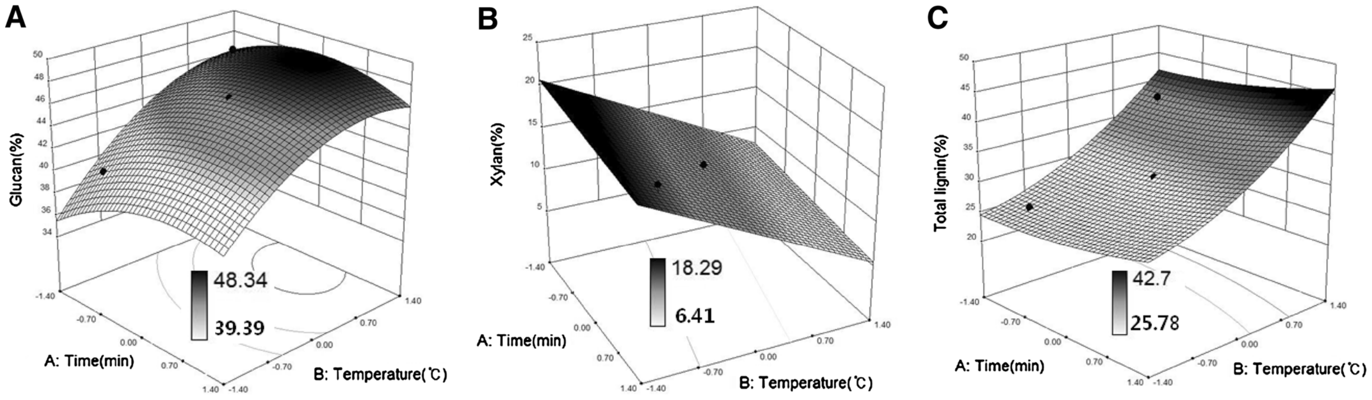

Fig. 2 Response surface and contour plot of temperature versus reaction time for the glucan, xylan, and lignin concentrations during torrefaction (**a** glucan, **b** xylan, and **c** lignin)

Table 4 Analysis of variance (ANOVA) for the adjusted model for glucan, xylan, and lignin in the biomass during torrefaction

Source	Sum of squares	*df*	Mean square	*F* value	*p* value (Prob > *F*)
Glucan					
Model	95.92	5.00	19.18	39.85	0.0005
Residual	2.41	5.00	0.48		
Lack of fit	2.18	3.00	0.73	6.34	0.14
Pure error	0.23	2.00	0.11		
Corrected total	98.32	10.00			
Temp.	76.53	1.00	76.53	158.99	<0.0001
Time	4.30	1.00	4.30	8.94	0.03
Time × temp.	1.18	1.00	1.18	2.45	0.18
$(\text{Temp.})^2$	11.14	1.00	11.14	23.14	0.00
$(\text{Time})^2$	6.61	1.00	6.61	13.74	0.01
Adjusted R^2: 0.9755					
Xylan					
Model	171.41	2.00	85.71	99.69	<0.0001
Residual	6.88	8.00	0.86		
Lack of fit	5.87	6.00	0.98	1.95	0.38
Pure error	1.00	2.00	0.50		
Corrected total	178.29	10.00			
Temp.	164.10	1.00	164.10	190.88	<0.0001
Time	7.31	1.00	7.31	8.50	0.02
Time × temp.	6.88	8.00	0.86	0.00	0.00
$(\text{Temp.})^2$	5.87	6.00	0.98	1.95	0.38
$(\text{Time})^2$	1.00	2.00	0.50	0.00	0.00
Adjusted R^2: 0.9614					
Lignin					
Model	348.37	5.00	69.67	76.73	0.0001
Residual	4.54	5.00	0.91		
Lack of fit	4.22	3.00	1.41	8.70	0.10
Pure error	0.32	2.00	0.16		
Corrected total	352.91	10.00			
Temp.	321.93	1.00	321.93	354.54	<0.0001
Time	14.23	1.00	14.23	15.67	0.01
Time × temp.	0.03	1.00	0.03	0.03	0.87
$(\text{Temp.})^2$	12.12	1.00	12.12	13.35	0.01
$(\text{Time})^2$	1.63	1.00	1.63	1.80	0.24
Adjusted R^2: 0.9871					

$$Y_3 = 31.2733 + 6.3436x_2 + 1.3336x_1 + 0.08x_1x_2 + 1.4652x_2^2 + 0.5377x_1^2 \quad (4)$$

The glucan contents in the biomass depending on reaction temperature and time are shown in Fig. 2a. According to the model, temperature and time squared were the only significant parameters. The reaction temperature had more impact on the change of glucan content than the reaction time during torrefaction under the studied conditions. The glucan concentration increased with increasing temperature and time, but decreased under severe conditions with high temperatures and long reaction times. This finding implies that cellulose degradation begins under severe conditions (Lee et al. 2012). The xylan concentration during torrefaction depended highly on reaction temperature rather than time (Fig. 2b). Low xylan concentrations were observed at high reaction temperature and long reaction time. The lignin concentration significantly increased at high temperature because of cellulose and hemicelluloses degradation during torrefaction (Fig. 2c). The reaction temperature had the highest impact on the lignin concentration in the torrefied biomass; time had a considerably lower effect.

The proposed model for determining the chemical compositions was validated under the conditions determined by the statistical methodology. Torrefaction was conducted at high SF (0.7–1.4 code level of temperature and time for glucan and lignin in Fig. 2). However, the energy yield should be considered to determine the optimal torrefaction condition.

Analysis of caloric value and weight loss based on SF

Calorific value and weight loss depending on SF are shown in Fig. 3. The calorific value and weight loss gradually increased with SF. The change in the carbon, glucan, and lignin contents in the biomass, depending on SF, was correlated with the calorific value. This result is in agreement with that of other studies (Lee et al. 2012;

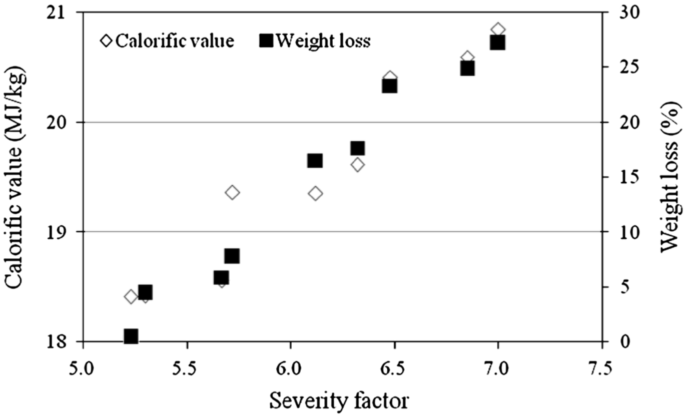

Fig. 3 Calorific value and weight loss of torrefied biomass depending on torrefaction severity

Medic et al. 2012). The calorific value of the torrefied biomass was 20.84 MJ/kg at an SF of 7.0, representing an increase of 15.01 % compared to the raw material. The weight loss of the biomass is an important indicator of the degree of torrefaction (Ohliger et al. 2013). The weight loss of biomass also increased with increasing SF. At SF 7, the biomass lost more than 27 % of the raw material weight. At low SF, the weight loss mostly resulted from the thermal degradation of hemicelluloses and the release of volatile components from biomass, whereas the weight loss of biomass at high SF was attributed to the simultaneous reactions of hemicelluloses and cellulose (Lee et al. 2012). The calorific value and weight loss did not change concurrently; the weight was lost faster than the calorific value. Therefore, severe torrefaction conditions are desirable for biomass with high energy density, such as that with high glucan and lignin content.

Physical characterization of torrefied biomass

In general, wood chips and pellets have relatively high moisture contents, hydrophilic behavior, and storage issues when compared with coal (Chen and Kuo 2010). Therefore, hydrophobicity is required for biomass transported over long distances and stored for a long time. The hydrophobicity of the torrefied biomass results in less moisture uptake during storage. Figure 4 shows that the moisture uptake capacity of torrefied biomass depended on the SF. Moisture uptake capacity decreased with increasing torrefaction severity. The low moisture uptake capacity indicates that the biomass was highly hydrophobic. This finding is in agreement with other reports (Ibrahim et al. 2013; Satpathy et al. 2014). In particular, the moisture concentration sharply decreased at SF 5.72 and then gradually decreased because the volatile compounds and hemicelluloses were preferentially removed during torrefaction at low SF.

Torrefaction provides improvement of the physical properties of biomass by increasing the hydrophobicity. However, this property negatively affects the pelletizing of the torrefied biomass.

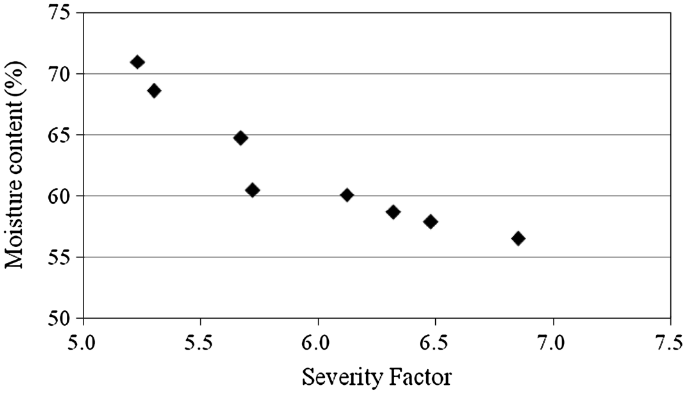

Fig. 4 Moisture uptake capacity of torrefied biomass measured by water immersion

The effect of the torrefaction SF on the particle size distribution of ground torrefied biomass through three different sieves is shown in Fig. 5. The torrefaction at a high SF produced smaller particles than mild torrefaction. The large particle size (>1 mm) decreased with increasing SF. As the torrefaction severity increased, the torrefied biomass became more grindable or brittle, resulting in a higher fraction of the sample passing through the 0.25-mm sieve. The torrefaction severity plays an important role in determining the size distribution. A similar trend of particle size distribution has also previously been reported (Phanphanich and Mani 2011; Chen and Kuo 2010). Overall, the torrefied biomass presented a relatively uniform particle size range relative to the raw material because the torrefied biomass is easily broken, similar to coal. This behavior was directly supported by the grinding energy consumption of the torrefied biomass for pellet production.

To produce pellets from torrefied biomass, size reduction in the biomass is required. The energy consumption needed for size reduction was estimated using a modification of a previous method (Phanphanich and Mani 2011). The effect of the torrefaction conditions on the power consumption required for grinding of the torrefied biomass and raw material is shown in Fig. 6. The torrefied biomass (55.1–65.6 kWh/t) required significantly less energy for size reduction than the raw material (145 kWh/t), resulting in energy savings of 54.7–62 %. The specific grinding energy consumption of torrefied biomass decreased with increasing severity, which was similar to the finding for particle production in the grindability test. Based on energy consumption, torrefied biomass is an economically feasible source for pellet production.

FT-IR spectra of raw material and torrefied biomass are shown in Fig. 7. Torrefied biomass changed significantly in the proximity of the 3,400 and 1,740–1,710 cm^{-1}. Bands at approximately 1,740–1,710 cm^{-1} are related to the stretching vibrations of the C=O groups of carboxylic acids within hemicelluloses

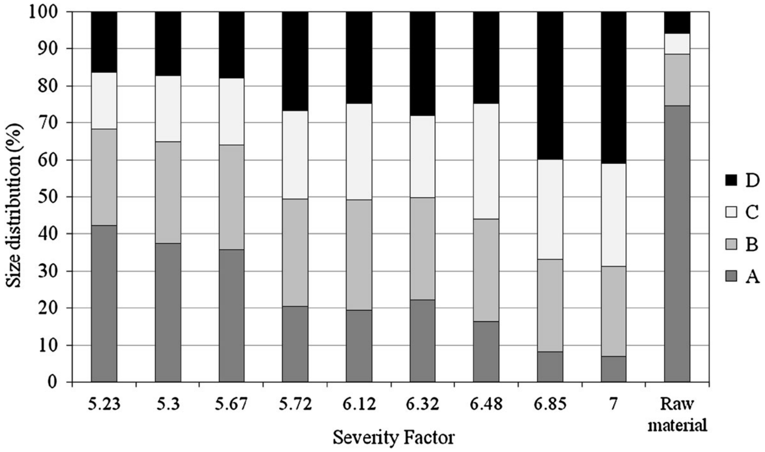

Fig. 5 Particle size distribution of torrefied biomass after grinding at various SF (*A* ∼1, *B* 0.425–1, *C* 0.25–0.425, *D* ∼0.25 mm)

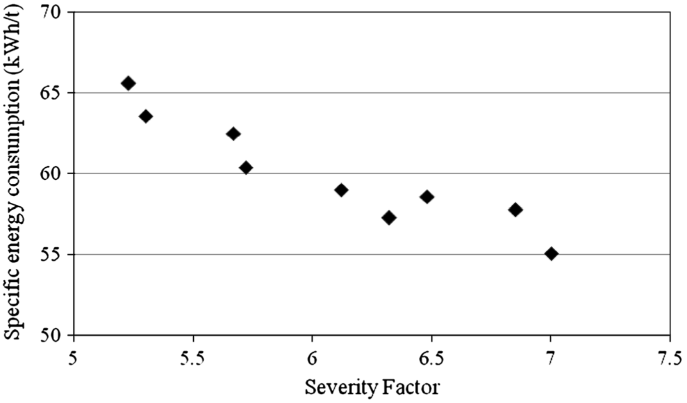

Fig. 6 Energy consumption for size reduction in raw material and torrefied biomass during grinding

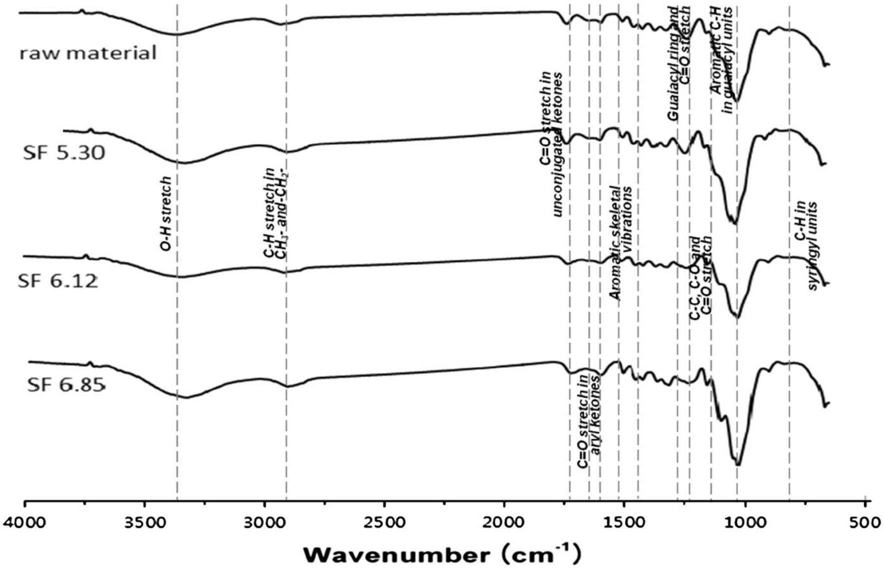

Fig. 7 Change of the FT-IR spectra in raw material and torrefied biomass depending on the torrefaction conditions

(Ibrahim et al. 2013). The intensity of the O–H bands decreased at approximately 3,400 cm^{-1}. The loss of O–H groups explains the improved hydrophobicity of torrefied biomass (Rousset et al. 2011). The peak at approximately 1,100 cm^{-1} (an aromatic C–H group) was present in both the raw material and torrefied biomass, indicating that lignin did not degrade under torrefaction conditions. At SF 6.85, the intensity of the C–O–C band (1,250–1,220 cm^{-1}) decreased, which is an indication that hemicelluloses and cellulose decomposed under severe torrefaction conditions.

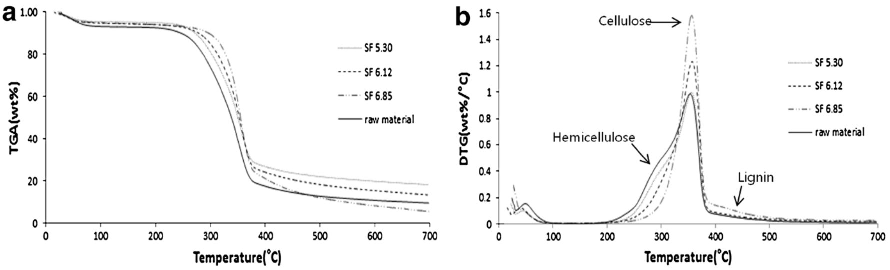

Fig. 8 Thermogravimetric analysis of raw material and torrefied biomass depending on the torrefaction conditions (**a** TGA, **b** DTG)

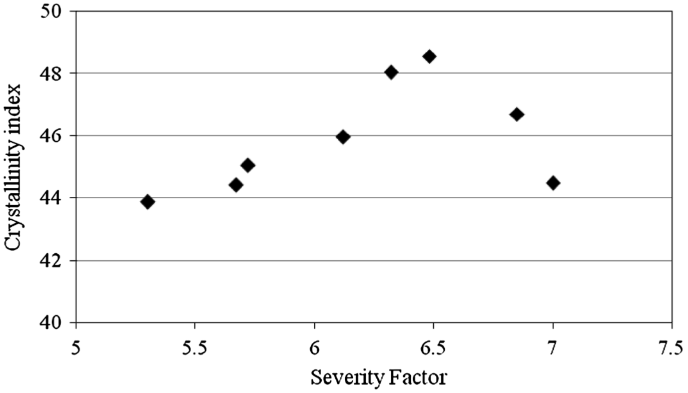

Fig. 9 Change in the crystallinity value of raw material and torrefied biomass

The TGA and DTG profiles of the raw material and torrefied biomass are shown in Fig. 8. The thermal decomposition behavior showed an obvious difference between raw material and torrefied biomass. Thermal decomposition was significantly accelerated between approximately 280 and 380 °C. The weight of the raw material decreased markedly at 250 °C, while the temperature for torrefied biomass increased with increased SF. In the derivative thermogravimetric (DTG) curve, the composition of hemicelluloses, cellulose, and lignin was clearly identified between raw material and torrefied biomass. The peak corresponding to hemicelluloses (305 °C) disappeared with increased SF. However, peaks representing cellulose (374 °C) and lignin (438 °C) increased significantly with increased SF. This is due to the pronounced degradation of hemicelluloses during torrefaction (Chen et al. 2011; Kim et al. 2012).

The cellulose crystalline structure in the biomass was changed by torrefaction. The crystallinity value of the raw material was estimated to be 35.83 %, while that of torrefied biomass ranged from 43.83 to 48.57 % (Fig. 9). The crystallinity value increased from 35.83 to 48.57 % until SF reached 6.48 due to degradation of hemicelluloses during torrefaction. The value drops to 44.47 % at a SF of 7. The increased crystallinity values of torrefied biomass are attributed to the degradation of amorphous hemicelluloses and amorphous regions of cellulose (Chang et al. 2012). Some of the crystalline cellulose in biomass decreased during severe torrefaction conditions (SF 7.0), which causes a decrease in the crystallinity of torrefied biomass.

Conclusion

The chemical and physical properties of torrefied biomass were investigated for different reaction temperatures and times. Reaction temperature had a strong impact on the change of the chemical composition of the torrefied biomass, whereas time had a considerably lower effect. At a low SF, torrefaction had a significant effect on the degradation of hemicelluloses, but not on that of cellulose or lignin. Torrefied biomass is more hydrophobic and becomes easier to grind to a small particle size. The specific grinding energy consumption of the torrefied biomass decreased with increasing torrefaction severity. Overall, the chemical and physical properties of torrefied biomass as fuel were improved compared to that of raw material.

Acknowledgments This work was supported by Priority Research Centers Program through the National Research Foundation of Korea (NRF) funded by the Ministry of Education, Science and Technology (Project No. 2010-0020141).

References

Bergman PCA, Boersma AR, Zwart RWR, Kiel JHA (2005) Torrefaction for biomass co-firing in existing coal-fired power stations. ECN Biomass, pp 13–17

Bourgeois J, Bartholin MC, Guyonnet R (1989) Thermal treatment of wood; analysis of the obtained product. Wood Sci Technol 23:303–310

Chang S, Zhao Z, Zheng A, He F, Huang Z, Li H (2012) Characterization of products from torrefaction of sprucewood and bagasse in an auger reactor. Energy Fuels 26:7009–7017

Chen WH, Kuo PC (2010) A study on torrefaction of various biomass materials and its impacts on lignocellulosic structure simulated by a thermogravimetry. Energy 35:2580–2586

Chen WH, Hsu HC, Lu KM, Lee WJ, Lin TC (2011) Thermal pretreatment of wood (lauan) block by torrefaction and its influence on the properties of the biomass. Energy 36:3012–3021

Chin KL, H'ng PS, Go WZ, Wong WZ, Lim TW, Maminski M, Paridah MT, Luqman AC (2013) Optimization of torrefaction conditions for high energy density solid biofuel from oil palm biomass and fast growing species available in Malaysia. Ind Crops Prod 49:768–774

Gwak K, Kim H, Ryu K, Choi H, Cho D, Kim P, Choi I (2009) Growth improvement of *Liriodendron tulipifera* through SCB manure treatment. For Bioenergy 28:7–14

Ibrahim RHH, Darvell LI, Jones JM, Williams A (2013) Physicochemical characterization of torrefied biomass. J Anal Appl Pyrolysis 103:21–30

Kim YH, Lee SM, Lee HW, Lee JW (2012) Physical and chemical characteristics of products from the torrefaction of yellow poplar (*Liriodendron tulipifera*). Bioresour Technol 116:120–125

Klinger J, Bar-Ziv E, Shonnard D (2013) Kinetic study of aspen during torrefaction. J Anal Appl Pyrolysis 104:146–152

Korea Forest Service (2009) The quality standard of wood pellet. Korea Forest Research Institute, Seoul, pp 1–29

Lee S, Lee J (2014) Optimization of biomass torrefaction conditions by the gain and loss method and regression model analysis. Bioresour Technol 172:438–443

Lee J, Kim Y, Lee S, Lee H (2012) Optimizing the torrefaction of mixed softwood by response surface methodology for biomass upgrading to high energy density. Bioresour Technol 116:471–476

Lehtikangas P (2001) Quality properties of pelletised sawdust, logging residues and bark. Biomass Bioenergy 20:351–360

Lloyd TA, Wyman CE (2005) Combined sugar yields for dilute sulfuric acid pretreatment of corn stover followed by enzymatic hydrolysis of the remaining solids. Bioresour Technol 96:1967–1977

Medic D, Darr M, Shah A, Potter B, Zimmerman J (2012) Effects of torrefaction process parameters on biomass feedstock upgrading. Fuel 91:147–154

Ohliger A, Forster M, Kneer R (2013) Torrefaction of beechwood: a parametric study including heat of reaction and grindability. Fuel 104:607–613

Pala M, Kantarli IC, Buyukisik HB, Yanik J (2014) Hydrothermal carbonization and torrefaction of grape pomace: a comparative evaluation. Bioresour Technol 161:255–262

Peduzzi E, Boissonnet G, Haarlemmer G, Dupont C, Maréchal F (2014) Torrefaction modelling for lignocellulosic biomass conversion processes. Energy 70:58–67

Phanphanich M, Mani S (2011) Impact of torrefaction on the grindability and fuel characteristics of forest biomass. Bioresour Technol 102:1246–1253

Pimchuai A, Dutta A, Basu P (2010) Torrefaction of agricultural residues to enhance combustible properties. Energy Fuels 24:4638–4645

Prins MJ, Ptasinski KJ, Janssen FJJG (2006) Torrefaction of wood: part 2. Analysis of products. J Anal Appl Pyrolysis 77:35–40

Rousset P, Davrieux F, Macedo L, Perre P (2011) Characterisation of the torrefaction of beech wood using NIRS: combined effects of temperature and duration. Biomass Bioenergy 35:1219–1226

Sannigrahi P, Kim DH, Jung SK, Ragauskas A (2011) Pseudo-lignin and pretreatment chemistry. Energy Environ Sci 4:1306–1310

Satpathy SK, Tabil LG, Meda V, Naik SN, Prasad R (2014) Torrefaction of wheat and barley straw after microwave heating. Fuel 124:269–278

Segal L, Creely JJ, Martin AE, Conrad CM (1959) An empirical method for estimating the degree of crystallinity of native cellulose using the X-ray diffractometer. Text Res J 29:786–794

Shafizadeh F, Sarkanen KV, Tillman DA (1976) Thermal uses and properties of carbohydrates and lignins. Academic Press, New York

Sims REH, Hastings A, Schlamadingerz B, Taylor G, Smith P (2006) Energy crops: current status and future prospects. Glob Chang Biol 12:2054–2076

Sjöström E (1981) Wood chemistry: fundamentals and application. Academic press, New York

Wen J, Sun S, Yuan T, Xu F, Sun R (2014) Understanding the chemical and structural transformations of lignin macromolecule during torrefaction. Appl Energy 121:1–9